Journal of Hydrology: Regional Studies 36 (2021) 100837

Contents lists available at ScienceDirect

Journal of Hydrology: Regional Studies

journal homepage: www.elsevier.com/locate/ejrh

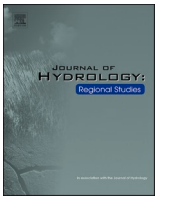

Improvement of the ESA CCI Land cover maps for water balance analysis in tropical regions: A case study in the Muda River Basin, Malaysia

Mou Leong Tan [a,*], Yi Lin Tew [a], Kwok Pan Chun [b], Narimah Samat [a], Shazlyn Milleana Shaharudin [c], Mohd Amirul Mahamud [a], Fredolin T. Tangang [d]

[a] GeoInformatic Unit, Geography Section, School of Humanities, Universiti Sains Malaysia, 11800 USM, Pulau Pinang, Malaysia
[b] Department of Geography, Hong Kong Baptist University, Hong Kong, China
[c] Department of Mathematics, Faculty of Science and Mathematics, Universiti Pendidikan Sultan Idris, Malaysia
[d] Department of Earth Sciences and Environment, Faculty of Science and Technology, Universiti Kebangsaan Malaysia, Bangi, Malaysia

ARTICLE INFO

Keywords:
Land use
SWAT
European Space Agency
Oil palm
Tropical
Malaysia

ABSTRACT

Study region: The Muda River Basin (MRB), Malaysia.
Study Focus: This study proposed a framework to improve the European Space Agency Climate Change Initiative Land Cover (ESA CCI LC) products through the integration with the Annual Oil Palm Dataset (AOPD). The improved land use land cover (LULC) maps were then used to produce five LULC scenarios as input maps into the Soil and Water Assessment Tool (SWAT) model for analyzing the impact of LULC changes on water balance in the MRB.
New hydrological insights for the region: The improved LULC maps have good performance in representing rubber and oil palm, with an overall accuracy up to 81 %. In addition, SWAT simulated monthly streamflow well for the MRB, with the highest R^2 and NSE values of 0.84 and 0.86, respectively. During the 2001–2016 period, the MRB experienced an expansion of oil palm from 7.10%–17.36 %, a reduction of rubber from 34.93 % to 26.38 % and a slight decrease in forest from 54.23%–52.80 %. The urban expansion scenario showed significant increment in surface runoff, while the reforestation scenario helped to reduce surface runoff, while increase lateral flow and groundwater. Oil palm expansion led to a higher reduction in lateral flow and groundwater than rubber trees due to the higher soil water absorption rate. The proposed framework can be duplicated and applied in other tropical basins, particularly in Indonesia and Malaysia.

1. Introduction

The accurate representation changing land use land cover (LULC) related to urbanization, agricultural expansion and deforestation is crucial for water resources management. The human population has increased significantly from ~2.6 billion people in 1950 to ~7.7 billion people in 2020, and is projected to increase another 2 billion people in the next 30 years (UN, 2020). In the long run, the population growth leads to increasing of global demand for urban land and agricultural products, which dramatic change the LULC

* Corresponding author.
E-mail address: mouleong@usm.my (M.L. Tan).

https://doi.org/10.1016/j.ejrh.2021.100837
Received 12 February 2021; Received in revised form 4 April 2021; Accepted 16 May 2021
Available online 25 May 2021

patterns. An extensive deforestation was observed in tropical region in the past few decades (Malingreau et al., 1989; Stibig et al., 2014). For instance, tropical forests have been logged to oil palm for fulfilling the huge demand of vegetable oils (Tapia et al., 2021). LULC plays a vital role in earth-atmosphere interactions that affecting water balance such as evapotranspiration, surface runoff and groundwater within a river basin system. Therefore, it is essential to quantify the effect of LULC changes on water balance, so that a better water resources management plan can be formulated.

Mapping of LULC pattern from time to time is essential as one of the major inputs in hydrological model to evaluate the LULC impacts on water balance at basin-scale (Nilawar and Waikar, 2018; Tamm et al., 2018; Tan et al., 2015). LULC maps are commonly prepared and released by local government, but sometime these maps are not available to the public due to the data restriction policy, lacking of infrastructure and expertise. With advances in the satellite and computer technologies, historical LULC maps can now be produced easily without relying on the government LULC data. However, modelers need to have a considerable knowledge and experience in satellite images processing in order to produce reliable LULC maps. For those with little or zero-knowledge in remote sensing, readily available global LULC products such as the Moderate Resolution Imaging Spectroradiometer (MODIS) Land Cover Type product (MCD12Q1) (Sulla-Menashe and Friedl, 2018), the Global Land Cover 2000 (GLC2000) (Bartholomé and Belward, 2005) and European Space Agency Climate Change Initiative Land Cover (ESA CCI LC) (Defourny et al., 2016), can be an alternative choice of getting LULC maps.

The ESA CCI LC products with 300 m spatial resolution and 27-year temporal data (1992–2018) have been widely used to monitor the global LULC changes (Mousivand and Arsanjani, 2019; Nowosad et al., 2019). At the basin scale, Chirachawala et al. (2020) compared several global LULC maps for simulating streamflow of the Upper Yom River Basin using the Soil and Water Assessment Tool (SWAT) and found that the ESA CCI LC product performed well in the annual flow, seasonal flow and baseflow simulations. However, Reinhart et al. (2021) noticed that the ESA CCI LC products unable to identify some LULC classes over Eastern Europe. In Malaysia, Kondo et al. (2021) reclassed the ESA CCI LC map manually based on the field survey and Google Earth satellite images before applying into SWAT to simulate streamflow and fecal contamination of the Selangor River Basin. Nevertheless, the authors didn't validate the modified map. To the best of our knowledge, an improvement of the ESA CCI LC maps for tropical basins that dominated with oil palm

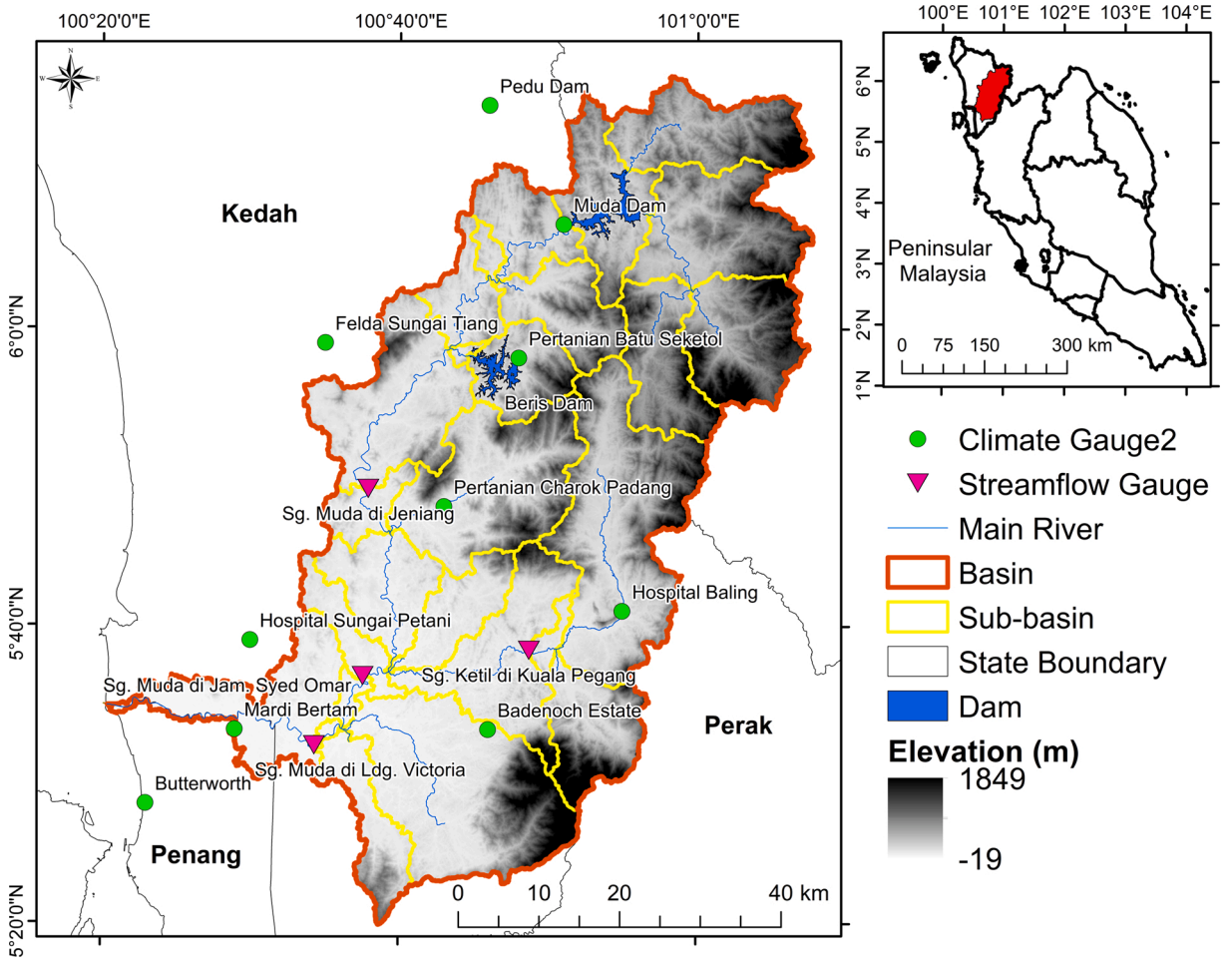

Fig. 1. Topography and distribution of the hydro-climatic gauges in the Muda River Basin, Malaysia.

and rubber is missing, and therefore, this study is conducted to tackle this issue.

SWAT has been proven to be a reliable hydrological model to study the impacts of LULC changes on water balance in different river basins around the world (Gassman et al., 2014; Gassman and Wang, 2015; Tan et al., 2019a). For instance, Schilling et al. (2008) quantified the water balance changes of the Raccoon River watershed in the west-central Iowa under several agricultural expansion scenarios for adaptive agricultural management decisions making. Tan et al. (2015) reported the conversion of forest to oil palm in the Johor River Basin that located in the southern Peninsular Malaysia increased surface runoff and lateral flow significantly while decreased groundwater and percolation. The Muda River Basin (MRB) is a transboundary tropical basin situated in the northern Peninsular Malaysia that supplies freshwater for irrigation, industry and domestic usage to three northern states of Pulau Pinang, Kedah and Perlis. Any dramatic LULC changes within the basin can affect the freshwater supply. However, quantification of the LULC changes on water balance of the MRB is still limited and need to be assessed.

Annual oil palm dataset (AOPD) from 2001 to 2016 generated by multiple satellite datasets (Xu et al., 2020) can be potentially used to integrate with the ESA CCI LC maps, so that the oil palm distribution can be better displayed. Hence, we proposed a framework to improve the ESA CCI LC maps by merging with the AOPD dataset. This improvement procedure does not require much remote sensing knowledge from the hydrology modeler. This study aims to evaluate the impact of LULC changes on water balance in the Muda River Basin (MRB), Malaysia, using the improved ESA CCI LC maps and SWAT. Three specific objectives of this study are: (1) to improve and validate the ESA CCI LC maps over the MRB; (2) to assess the spatio-temporal LULC changes of the MRB; (3) to evaluate the impact of LULC changes on water balance in the MRB. The novelty of this study is generation of a higher level LULC classification from the ESA CCI LC products in oil palm dominated tropical regions. The framework can be applied in other tropical basins, particularly in Indonesia and Malaysia.

2. Materials and methodology

2.1. Study area

The MRB has a drainage area of 4119.76 km^2, with the mean elevation of 245.95 m (Fig. 1). The total river length of Muda River is about 180 km. During the 1985–2015 period, mean maximum temperature of the MRB varied from 30.9–34.5 °C and mean minimum temperature of 21–21.35 °C (Tan et al., 2019b). Besides that, the basin receives around 2500 mm/year annual precipitation, with higher monthly precipitation amount from April to May and August to November, mostly more than 250 mm/month (Tan et al., 2019b). Whereas, a relative lower monthly precipitation amount (less than 100 mm/month) is normally found in January and February. Sometime, the drier condition may be extended to April or May due to the El Niño effect (Tangang et al., 2017). For example, the MRB experienced a long dry spell from January to June in 2020 which resulted the water level of few dams within and surrounding of the basin hit their history lowest level.

There are two dams within the MRB, the Muda Dam that located in the northern part of the basin, and the Beris Dam in the middle part, as shown in Fig. 1. The Muda dam has the capacity of 160 million m^3, and is mainly used for paddy irrigation purposes. Due to the low capacity, water from Muda Dam is transferred to a larger dam, called the Pedu Dam (1073 million m^3), through the 6.8 km long Saiong Tunnel (MADA, 2020). Muda Agricultural Development Authority (MADA) is the authority involves in the management and operation of the Muda Dam. The Beris Dam that completed in 2004 is managed by the Department of Irrigation and Drainage (DID) of Malaysia. With the capacity of 114 million m^3, it has similar functions as the Muda Dam.

2.2. SWAT inputs

Basic data for the SWAT setup include daily precipitation, daily maximum and minimum temperature, a digital elevation model (DEM), a land use map and a soil map. Daily climate data from eleven well distributed climate stations for the period of 1995–2019 were collected from the Malaysian Meteorological Department (MMD) (Fig. 1). Out of these stations, only the Muda Dam, Butterworth and Pusat Pertanian Charok Padang stations contain daily maximum and minimum temperature data. A 30 m DEM was collected from the Shuttle Radar Topography Mission (SRTM), while the Food and Agriculture Organization (FAO) soil map was used as the soil input in the SWAT modelling. As mentioned earlier, this study adopted the land use maps from the ESA CCI LC products, where the details information will be described in the next section. Monthly streamflow data for the 2000–2019 period were obtained from DID to calibrate and validate the SWAT model. Lastly, major river networks within the MRB were digitized from the Google Earth Pro satellite images to generate better river networks during the DEM-based river network formation produce.

2.3. Integration of the ESA CCI LC and AOPD products

The ESA CCI LC products were created for the purposes of climate modelling. Multiple satellite sensors such as Medium Resolution Imaging Spectrometer (MERIS), Envisat Advanced Synthetic Aperture Radar (ASAR), Advanced Very High Resolution Radiometer (AVHRR), Project for On-Board Autonomy - Vegetation (PROBA-V) and Satellite Pour l'Observation de la Terre - Vegetation (SPOT-VGT) (ESA, 2017) were used as the raw datasets in the products development. The GlobCover unsupervised classification approach was used to classify 37 LULC classes based on the FAO standard (Plummer et al., 2017). The overall accuracy of the ESA CCI LC 2015 map is 75.4 % when comparing to the GlobCover data (ESA, 2017).

The AOPD dataset was developed to evaluate the oil palm expansion in Indonesia and Malaysia. It is available at 100 m spatial resolution from 2001 to 2016. Numerous satellite sensors including Advanced Land Observing Satellite (ALOS), Phased Array type L-

band synthetic Aperture Radar (PALSAR), ALOS-2, PALSAR-2 and MODIS data were used in the AOPD formation (Xu et al., 2020). Basically, the AOPD development involves two major steps: (1) oil palm expansion mapping using PALSAR and PALSAR-2 for the 2007–2010 and 2015–2016 periods; and (2) updating the maps for the missing period of PALSAR from 2001 to 2006 and 2011–2014 using MODIS NDVI data with the Break for Additive Season and Trend (BFAST) algorithm. The overall accuracy of the AOPD maps is 86.61 % for the 2007–2010 and 2015–2016, and is 75.54 % for the remaining periods (Xu et al., 2020).

We proposed a framework to integrate the ESA CCI LC and AOPD products which required only some basic GIS knowledge from the modeller, since it can be done solely with the ArcMap or QGIS tool. Fig. 2 shows the research process flowchart of this study. The improved ESA CCI LC framework consists of seven major steps as follows:

Step 1: Download both the ESA CCI LC and AOPD products from their webpage at http://maps.elie.ucl.ac.be/CCI/viewer/download.php (ESA, 2017) and https://doi.org/10.5281/zenodo.3467071 (Xu et al., 2020), respectively.

Step 2: Extract study area from both the products. In this case, the products were clipped with the MRB boundary delineated via the watershed delineation function within SWAT.

Step 3: Resample of AOPD to the same spatial resolution of the ESA CCI LC maps.

Step 4: Reclass the ESA CCI LC classes based on the major LULC types that available in the study area. For MRB, 13 LULC classes from the original ESA CCI LC maps were reclassed to forest, agricultural, water, urban and paddy.

Step 5: Check the spatial distribution of each LULC class with local maps or Google Earth Pro satellite images, particularly for agricultural and forest. This step is essential to check whether the classes are correctly representing the actual situation. Based on our field survey and land use maps generated by the Department of Agricultural Malaysia, rubber and oil palm are the major crops in the MRB. Therefore, the ESA CCI LC agricultural classes are mostly treated as oil palm and rubber.

Step 6: Apply the Con tool under Spatial Analyst of ArcMap to integrate both the products. The raster pixel values of the ESA CCI LC maps that overlay with the oil palm distribution extracted from the AOPD maps were reclassed as oil palm. Meanwhile, the remaining agricultural pixels were reclassed as rubber.

Step 7: Validation of the improved ESA CCI LC maps using the overall accuracy and kappa coefficient approaches with the samples extracted from the reference maps, high-resolution satellite images from Google Earth Pro and/or field survey.

Accuracy assessment is a process of validating the classification effectiveness to represent the actual LULC (Foody, 2010; Lyons et al., 2018). The accuracy assessment of the improved ESA CCI land cover maps is done by first selecting the training samples, cross validating with the LULC maps and compute the error matrix. As suggested by Olofsson et al. (2014), the first step in accuracy assessment is identifying major errors in the classification result through a rough visualization before a detailed planning of sampling designs. A major constraint of the original ESA CCI LC maps in the MRB is hard to differentiate agricultural crops. The classification system adopted in the ESA CCI land cover product followed the vegetation definitions established by Food and Agriculture (FAO), that is challenging in terms of extracting more details tropical agricultural crops such as oil palm and rubber (Fig. 3). Referring to the FAO vegetation glossary that we found in the website http://www.fao.org/3/x0596e/X0596e01n.htm, permanent rainfed crops, herbaceous rainfed crops and mosaic cropland are different in terms of planting management. However, in our study area MRB, these land

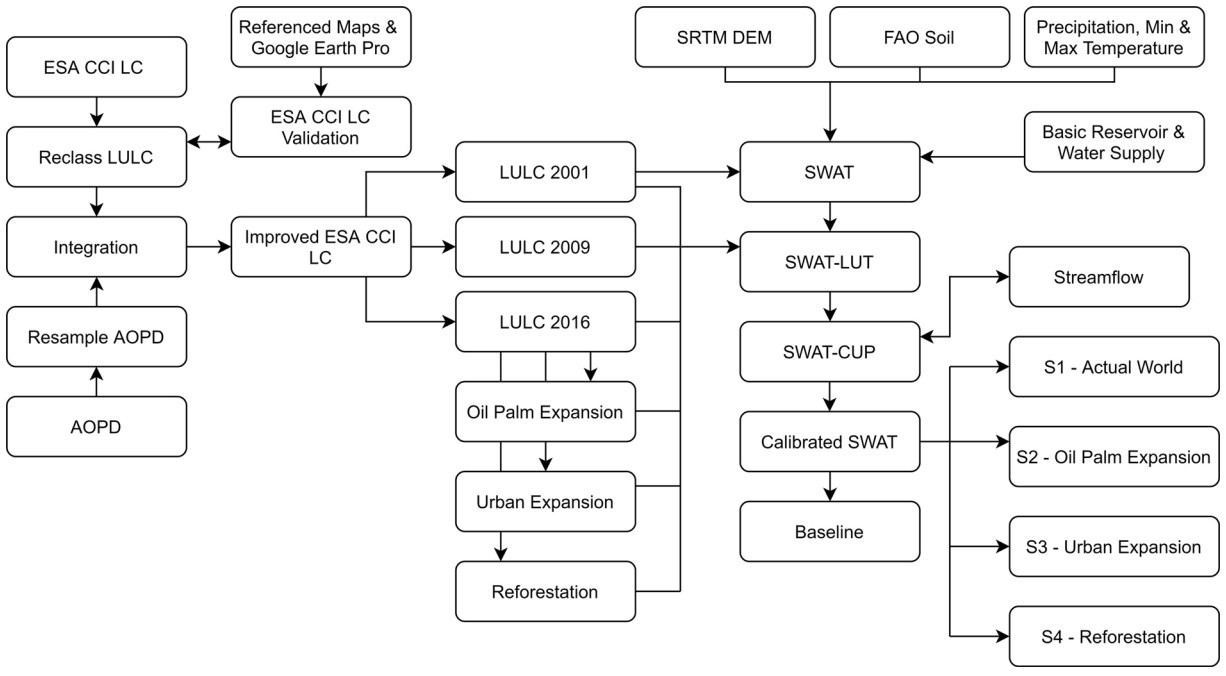

Fig. 2. Methodological flowchart to assess the impacts of land use land cover changes on tropical water balance using the improved ESA CCI LC maps and SWAT.

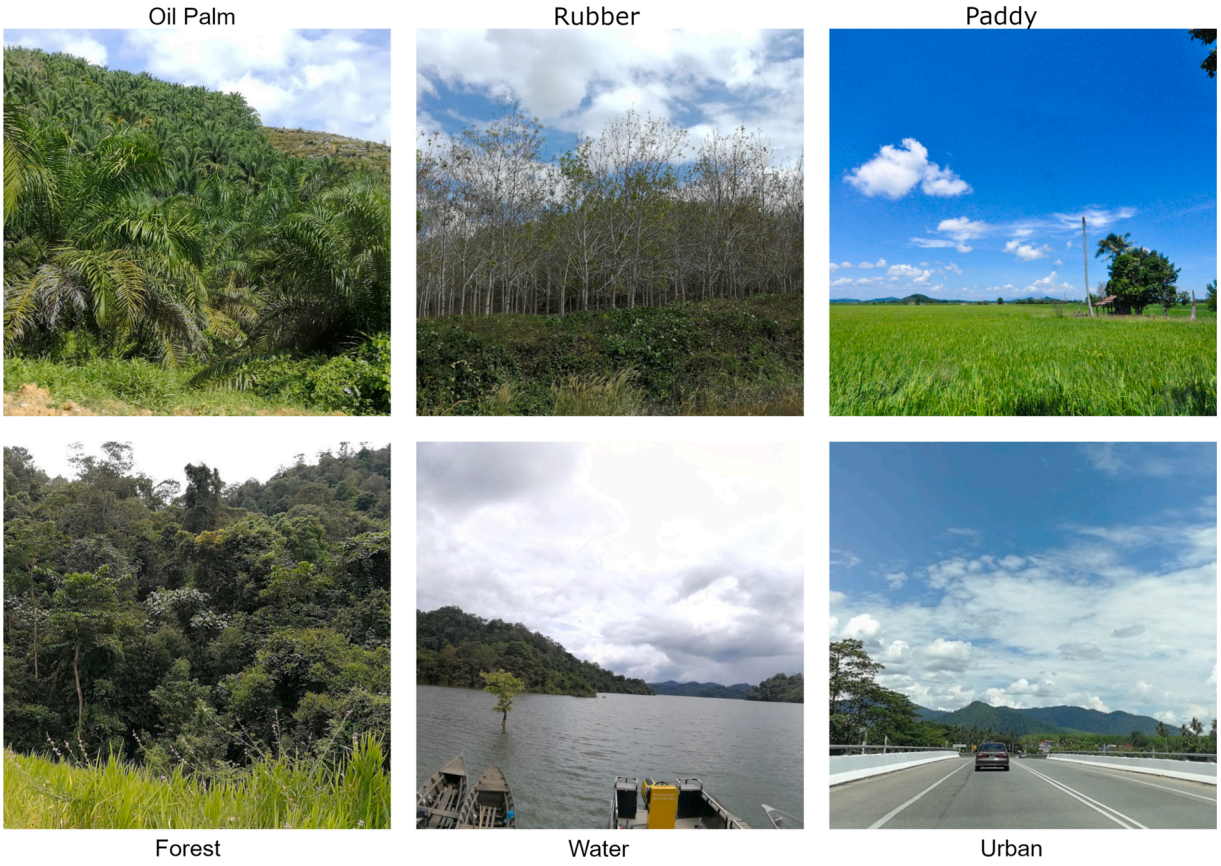

Fig. 3. Major types of land use land cover in the Muda River Basin, Malaysia.

cover class had mixed up with oil palm and rubber.

Independent samples collected from ground observations are commonly used as the training and test set input for sampling designs. Wulder et al. (2006) suggested that the sample size selection is dependent on the accepted minimum accuracy, often determined based on probability theory of the binomial distribution. A total of 60 random samples are selected for each class from the high-resolution Google Earth satellite images for validating the improved ESA CCI LC maps of 2009 and 2016, while the 2002 LULC map produced by the Department of Agricultural Malaysia was used to validate the 2001 map. Google Earth historical satellite data is a least-cost reliable source for ground truth sample collection as it can be zoomed into the ground-view extent, where it is almost similar to the in-situ field observations. With the local knowledge of the studied basin, we managed to generate more accurate sampling points for the accuracy assessment.

Accuracy assessment of the LULC products is done with the confusion matrix approach, where a cross-tabulation of the class label from the land cover product with the samples collected is computed (Foody, 2015). From the confusion matrix, the overall accuracy and the Kappa coefficient of the LULC products can be computed post hoc. This method is commonly practiced for classification results as the processes can be conducted with Excel and GIS software. The two indicators are derived as:

$$\text{Overall Accuracy} = \frac{No.\ of\ correctly\ matched\ pixels}{Total\ nummber\ of\ pixels}$$

$$\text{Kappa coefficient, } \kappa = \frac{P_o - P_e}{1 - P_e}$$

where P_o is the relative observed agreement among the raters and P_e is the hypothetical probability of chance agreement for each randomly observation (Cohen, 1960). κ ranges between 0–1, where the value can be interpreted by poor agreement: $\kappa < 0.20$, fair agreement: $0.20 < \kappa < 0.40$, moderate agreement: $0.40 < \kappa < 0.60$; good agreement: $0.60 < \kappa < 0.80$, very good agreement: $0.80 < \kappa < 1.00$. Thus, the overall accuracy of above 70 % and κ value of above 0.60 is considered as an acceptable result.

2.4. SWAT model

SWAT is a semi-distributed model developed by the United States Department of Agricultural (USDA) and the Texas A&M

University via the routing outputs to the outlet and integration of the simulator for water resources in rural basins models (Arnold et al., 1998). The model was designed to evaluate the impact of different management practices and human activities on water balance and river quality. A continuous model improvement since 1990s made it as one of the most powerful tools to analyze soil-water-waste nexus (Mannschatz et al., 2016). In addition, the model has been proven to be reliable in representing water balance, especially streamflow in different types of river basins around the world (Bressiani et al., 2015; Gassman et al., 2007; Tan et al., 2020, 2019a; van Griensven et al., 2012).

SWAT divides a basin into multiple sub-basins, and the sub-basins are further divided into smaller hydrological response units which run all the calculations. In this study, the minimum value of threshold for DEM based stream definition was set to 100 km^2, which resulted a total of 27 sub-basins. Then, the slope classes were divided into five major classes of 0–10 %, 10–20 %, 20–30 %, 30–40 %, and more than 40 %. The HRU threshold for land use, soil and slope was set to 10 %, which created a total of 326 HRUs. Basic information of the Muda and Beris Dams inserted to the SWAT model were obtained from the MADA (MADA, 2020) website and DID, respectively. In addition, average monthly water usage of MRB that collected from the National Water Balance Management System (NAWABS) (DID, 2020) and a report prepared by Van Kalken (2017) were also added to the SWAT model.

During the SWAT simulation, a five-year warm up period from 1995 to 1999 was given to initiate the soil water condition. Then, the remaining simulation was divided into the calibration (2000–2009) and validation (2010–2019) to evaluate the model performance before applying for the LULC impact assessment. Monthly streamflow data as mentioned in the section 2.2 were used for model calibration and validation. The sequential uncertainty fitting algorithm (SUFI-2) within the SWAT-CUP tool was used to calibrate the SWAT model, with 500 different parameters combinations (Abbaspour et al., 2018). The coefficient of determination (R^2) and Nash-Sutcliffe Efficiency (NSE) were used to evaluate the capability of SWAT in simulating monthly streamflow in MRB. The R^2 and NSE values range from 0 to 1 and -∞ to 1, respectively, with 1 as the optimal value. Negative NSE values indicate an unacceptable performance of the SWAT model. Based on the Moriasi et al. (2015), a "very good" model should obtain more than 0.85 for R^2 and 0.8 for NSE. Meanwhile, the R^2 and NSE values for "good" model should be more than 0.75 and 0.65, respectively.

2.5. Land use scenario analysis

We generated three historical LULC maps of 2001, 2009 and 2016 using the improved ESA CCI LC framework that described in the section 2.3. Although the ESA CCI LC maps are available every year from 1992 to 2018, but only three historical maps were generated due to the limited historical reference LULC maps for the accuracy assessment. In addition, LULC usually does not have significant changes within few years unless there are some land use policies that can cause abrupt the sudden changes. Furthermore, land use maps at decadal intervals are commonly used in the LULC impact assessment (Chen et al., 2020; Githui et al., 2009). Therefore, the improved 2001, 2009 and 2016 maps should be sufficient for the assessment of LULC impact on water balance in the MRB.

Table 1 lists five LULC scenarios generated from the improved ESA CCI LC maps. These LULC scenarios consists of a baseline map that used to compare with the other four different LULC scenarios. S1 scenario represents the actual LULC changes in MRB, while the other three LULC scenarios indicate the oil palm expansion, urban expansion and reforestation. The SWAT- Landuse Update Tool (SWAT-LUT) developed by Moriasi et al. (2019) was used to update the land use changes module within SWAT. SWAT-LUT is an improved version of SWAT2009_LUC (Pai and Saraswat, 2011) which can only be used to activate the land use module of the SWAT 2009 version. The SWAT-LUT tool is compatible with the SWAT 2012 (Revision 635) that used in this study.

Moriasi et al. (2019) recommended to activate the land use module for updating the LULC changes within SWAT using the SWAT-LUT before the calibration and validation (Fig. 2). Hence, the SWAT model for the MRB was initially created using the baseline land use map. Then, the LULC maps for the other four scenarios were incorporated into SWAT via the SWAT-LUT and stored to the respective SWAT project files. Next, the baseline SWAT model was used in the calibration and validation. Once the SWAT performance reached to a certain acceptable level, the same calibrated parameters were then transferred to other SWAT projects that have been activated with different LULC scenarios. Using the same calibrated parameters for all LULC scenarios SWAT projects is essential to minimize the parameter uncertainty in the modelling outputs.

3. Results

3.1. LULC analysis

The accuracy assessment of all the three improved LULC maps are presented in Table 2. In general, the improved ESA CCI LC maps performed well, with the overall accuracy values of 56 %, 81 % and 70 % for 2001, 2009 and 2016, respectively. This may be caused by

Table 1
Land use Scenarios.

Symbol	Scenario	Description
Baseline	Baseline for comparison	2001
S1	Actual world	2001, 2009, 2016
S2	Oil Palm Expansion	2016 – convert rubber to oil palm
S3	Urban Expansion	2016 – convert oil palm to urban & rubber to oil palm
S4	Reforestation	2016 – rubber to forest

the limitations of the vegetation definitions in representing vegetation covers in a tropical region, where the vegetation characteristics under the tropical climate may be different from other countries. Besides that, the Kappa coefficient of the original dataset is relatively low, where the statistical test shown that the dataset is at fair agreement for its classification system.

The confusion matrix of the improved LULC map for 2016 is tabulated in Table 3. Based on the constructed confusion matrix, the omission and commission errors for each of the designed land cover class are relatively high, especially for urban class. One of the reasons behind may be the dataset resolution factor that shall be considered during the sampling design. The urban areas covered a relatively small portion of the MRB (approximately 0.8 %), thus the samples collected from high resolution satellite data might fall onto the neighbouring pixels in the ESA CCI LC product.

Basically, about 50 % of the MRB is covered with forest, followed by rubber, oil palm, paddy, water and urban. Fig. 3 indicates some photos of the major land use types within the basin that taken during our field trip. Spatio-temporal changes of LULC over the MRB for the periods of 2001, 2009 and 2016 are shown in Figs. 4 and 5. There has been an increment in the oil palm plantations in the downstream MRB from 7.10%–17.36 % of the total basin size between 2001 and 2016. By contrast, rubber that dominated in the western and southern parts of MRB were reduced from 34.93 % in 2001 to 26.8 % in 2016. Paddy is distributed mainly near to the basin's outlet, ranging from 2.04 to 3.03 %. Meanwhile, forest within MRB is mainly found in the northern and southeastern parts, with a slight decrease in coverage area from 54.23%–52.80 %.

3.2. SWAT calibration and validation

The SWAT calibration parameters adopted by Zhang et al. (2020a) who tested the reliability of different climate data on SWAT outputs of the same basin were used in this study. A recalibration of SWAT was conducted since the authors ran the model for a shorter period of 2009–2014. By contrast, this study calibrated and validated SWAT for the periods of 2000–2009 and 2010–2019, respectively. Table 4 indicates the ranges and optimal values of the SWAT calibration parameters for the MRB. Similarly, SCS runoff curve number f (CN2), soil evaporation compensation factor (ESCO) and groundwater "revap" coefficient (GW_REVAP) are among the most sensitive parameters in the MRB (Zhang et al., 2020a).

The performance of SWAT in simulating monthly streamflow at four different streamflow gauges is presented in Fig. 6. Overall, SWAT had a "good" performance during the calibration as the R^2 and NSE values were above 0.7 at three streamflow gauges. The only "not satisfactory" performance was found in the Sg. Muda at Jeniang station, which may be due to the reservoir effects, but it is still under an acceptable performance as suggested by Moriasi et al. (2015). During the validation period, a "very good" SWAT performance can be found in the Sg Muda at Ladang Victoria station that nearest to the basin's outlet, with the R^2 and NSE values of 0.83 and 0.86, respectively. Another outstanding performance of SWAT can be observed in the Sg. Muda at Jambatan Syed Omar station ($R^2 = 0.84$ and NSE = 0.72). SWAT performed better during the validation period in the Sg. Muda at Jeniang station ($R^2 = 0.63$ and NSE = 0.47) than the calibration period. In contrast, a poorer performance was at the Sg. Ketil at Kuala Pegang station for the validation period, which may be due to the underestimation of peak flows.

3.3. Streamflow changes under different LULC scenarios

The effect of different LULC scenarios on the annual and monthly streamflow pattern at four streamflow stations and the basin's outlet for the period of 2000–2019 is shown in Fig. 7. The actual LULC, oil palm expansion, and urban expansion led to slightly changes of annual streamflow from -0.06 to 0.25 %, -0.59 to -0.03 % and -0.32 to 0.93 %, respectively. Table 5 shows only the oil palm expansion scenario resulted a reduction in annual streamflow, whereas the other three scenarios increased the annual streamflow. The reforestation scenario showed the largest increment in annual streamflow by 1.35 %, followed by the urban expansion (0.87 %) and actual (0.11 %) scenarios.

During the low flow period in January, February and March, monthly streamflow at the basin's outlet mostly decreased under all the evaluated LULC scenarios, with the urban expansion scenario had the greatest reduction rate. Fig. 7(e) shows that monthly streamflow in January and February under the urban expansion scenario decreased by 8.45 % (6.72 m^3s^{-1}) and 8.24 % (5.52 m^3s^{-1}), respectively. Reforestation is the only scenario increased monthly streamflow during the SWM season, from May to September by 1.00–3.12%. During the high flow or flood period, the urban expansion scenario caused the highest increment in monthly streamflow of August, September, October and November by 4.42 %, 7.27 %, 5.64 % and 3.77 %, respectively. A similar situation can be found at the Sg. Muda at Jambatan Syed Omar and Sg. Muda at Ladang Victoria stations. This indicates that rapid urbanization could increase the flood risk in the downstream part of MRB.

Table 2
Overall accuracy (OA) and Kappa coefficient (k) for the improved ESA CCI LC product.

Year	Overall Accuracy (%)	k
2001	56	0.47
2009	81	0.77
2016	70	0.64

Table 3
Confusion matrix of the improved ESA CCI LU product in 2016.

Y2016	V_OILP	V_RUBR	V_RICE	V_FRSE	V_URBN	V_WATR	Validated
OILP	46	2	2	14	13	9	86
RUBR	1	41	0	4	12	8	66
RICE	1	4	58	1	1	3	68
FRSE	1	13	0	36	4	0	54
URBN	1	0	0	5	30	0	36
WATR	10	0	0	0	0	40	50
Total	60	60	60	60	60	60	360

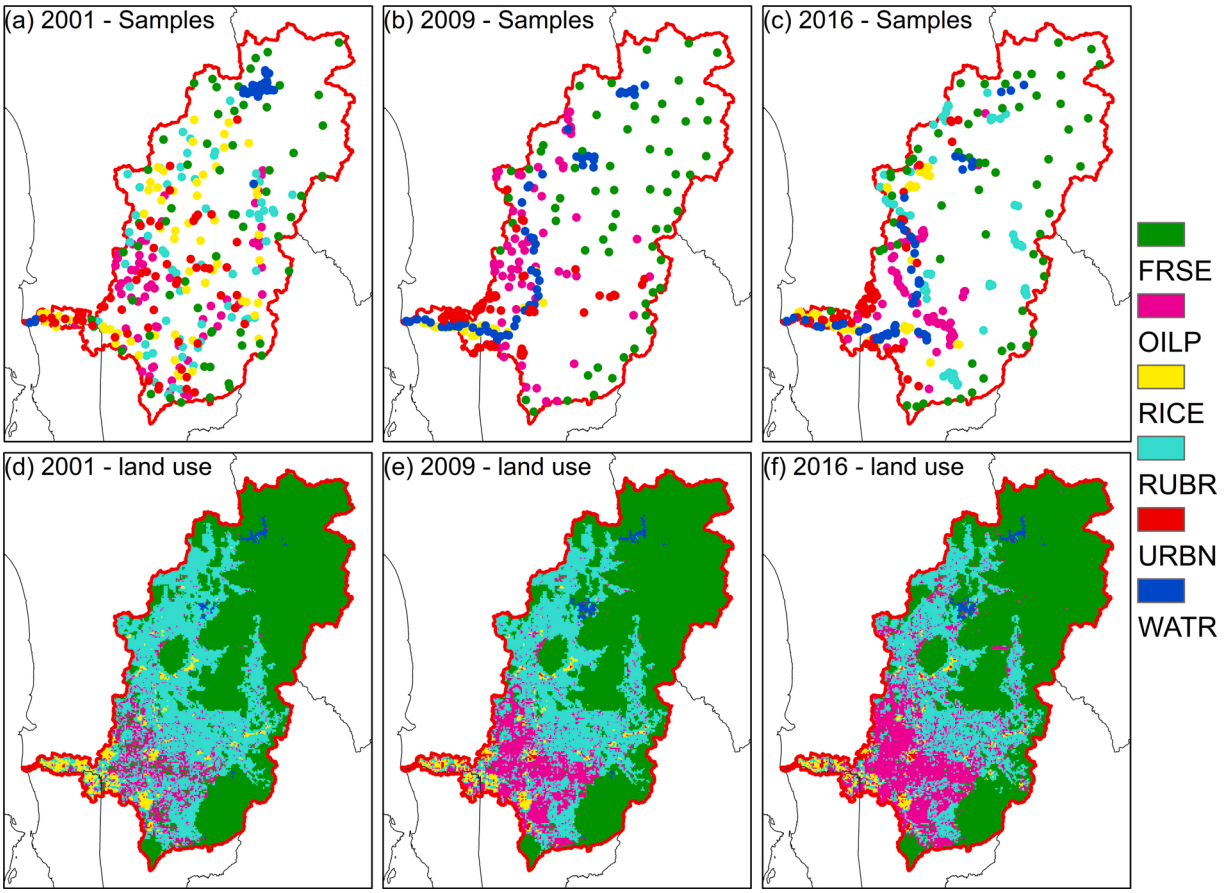

Fig. 4. The locations of the ground samples for (a) 2001, (b) 2009 and (c) 2016 and the spatial distribution of land use land cover of the Muda River Basin in (d) 2001, (e) 2009 and (f) 2016 that was extracted from the improved ESA CCI maps.

3.4. Water balance changes under different LULC scenarios

The response of annual surface runoff, lateral flow, groundwater, evapotranspiration, potential evapotranspiration and water yield as simulated using the calibrated SWAT under four land use scenarios from 2000–2019 in the MRB is shown in Fig. 8. It can be seen from Fig. 8 and Table 5 that LULC had a larger impact on annual surface runoff, lateral flow and groundwater as compared to evapotranspiration, potential evapotranspiration and water yield in this tropical basin.

Annual surface runoff increased significantly by 34.51 % when all oil palm plantations changed to urban area. Average monthly surface runoff also increased dramatically under the urban expansion scenario by 25.08%–59.76%, whereas the reforestation scenario reduced monthly surface runoff from 7.04%–10.20 % (Fig. 9a). The findings indicated that forest plays an important role in mitigating the flood impact in the MRB. On the other hand, the actual LULC and agricultural expansion scenarios only have a minor impact on monthly surface runoff simulation, which is less than 1.78 %.

Annual lateral flow decreased by 0.90–4.17% under all the LULC scenarios, except for the reforestation scenario which had an opposite direction of increment around 15.24 % (Table 5). Fig. 9(b) shows monthly lateral flow under the reforestation scenario

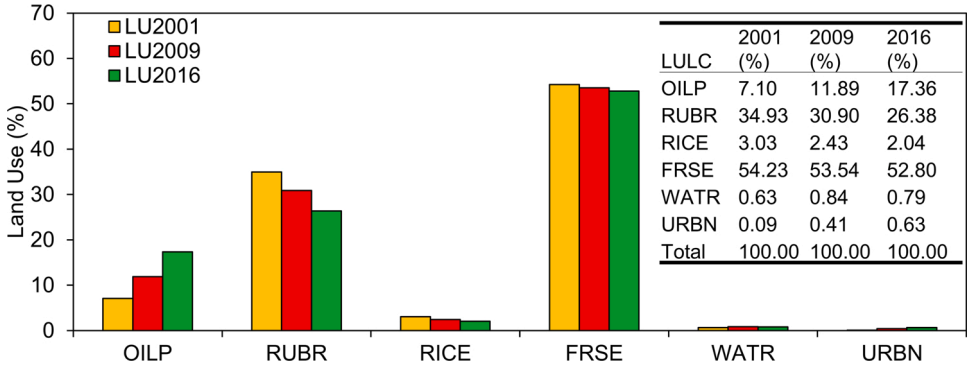

Fig. 5. Temporal changes of land use land cover of the Muda River basin from 2001 to 2016.

Table 4
SWAT calibration parameters (1 – most sensitive) for Muda River Basin, Malaysia.

No	Parameter	Name	Min	Max	Optimal
1	R_CN2.mgt	SCS runoff curve number f	−0.5	0.5	−0.19
2	V_ESCO.hru	Soil evaporation compensation factor	0	1	0.79
3	V_GW_REVAP.gw	Groundwater "revap" coefficient	0.02	0.2	0.14
4	R_SOL_Z(..).sol	Depth from soil surface to bottom of layer	−0.5	0.5	−0.05
5	R_HRU_SLP.hru	Average slope steepness	−0.5	0.5	0.07
6	R_SOL_BD(..).sol	Moist bulk density	−0.5	0.5	0.26
7	R_SOL_AWC(..).sol	Available water capacity of the soil layer	−0.5	0.5	−0.22
8	R_SLSUBBSN.hru	Average slope length	−0.5	0.5	0.22
9	R_SOL_K(..).sol	Saturated hydraulic conductivity	−0.5	0.5	0.05
10	V_RCHRG_DP.gw	Deep aquifer percolation fraction	0	1	0.61
11	V_GW_DELAY.gw	Groundwater delay (days)	0	500	317.50
12	V_CANMX.hru	Maximum canopy storage	0	10	8.81
13	V_CH_N2.rte	Manning's "n" value for the main channel	0	0.3	0.28

increased from 12.75 % to 17.00 %, respectively. Meanwhile, the urban expansion scenario caused a reduction in monthly lateral flow between 2.90 % and 5.38 %. Overall, the findings indicated that water movement within soil is largely affected by the types of LULC. Decreases of annual lateral flow under the actual LULC and oil palm expansion scenarios could be due to the water consumption of oil palm is higher than rubber (Hardanto et al., 2017). Oil palm absorbs more water within soil since its fibrous root system can spread over 25 m horizontally and 6 m vertically (Jourdan et al., 2000). In contrast, the root system of rubber trees only able to extend about 13 m horizontally and 3 m vertically.

The SWAT-simulated average annual groundwater of MRB is about 157.49 mm/year, which is consistent with the fact of 6 % of the total rainfall can be considered as the groundwater recharge rate in Malaysia (FOMCA, 2009). Annual groundwater had the greatest reduction rate under the urban expansion (18.84 %) scenario, followed by the actual LULC (5.80 %) and oil palm expansion (2.78 %) scenarios. Table 5 shows that reforestation managed to increase annual groundwater of the MRB by 6.38 %. Fig. 9(c) indicates that a higher monthly groundwater reduction is mainly found in the dry period such as March and June. Urban expansion is still causing the greatest reduction in monthly groundwater. This might be explained by the fact of expansion in concrete surfaces, pavements and buildings increased surface runoff as shown in Fig. 9(a). The impervious surfaces reduced the infiltration rate dramatically in the middle part of the MRB.

4. Discussion

The ESA CCI LC products have undergone some validation works, but mainly on global scale with 75.1 % accuracy for 2015 (ESA, 2017; Reinhart et al., 2021). In fact, some differences of LULC information can be still observed when comparing to other types of LULC products. For example, the ESA CCI LC product estimated the global total forest area in 2000 as 30.01 million km^2 (Li et al., 2016), which is lower than the values reported by Hansen et al. (2010) (32 million km^2) and FAO (2010) (40.85 million km^2). In the initial stage of this study, we noticed that the distribution of the original croplands from the ESA CCI LC products matches quite well with the actual cropland distribution within MRB. However, it is difficult to differentiate the oil palm and rubber accurately. Several attempts have been tried to reclass the cropland categories based on the major crops and their characteristic in MRB, but the results showed that the ESA CCI LC products mixed up the oil palm and rubber trees. This shows the ESA CCI LC products unable to provide a higher level LULC classification that required for a local scale analysis. A possible explanation for this might be that low number of observations over Malaysia in the MERIS archive (ESA, 2017). The improved ESA CCI LULC maps are useful to reduce the cropland mismatch issue that normally occurred in tropical regions.

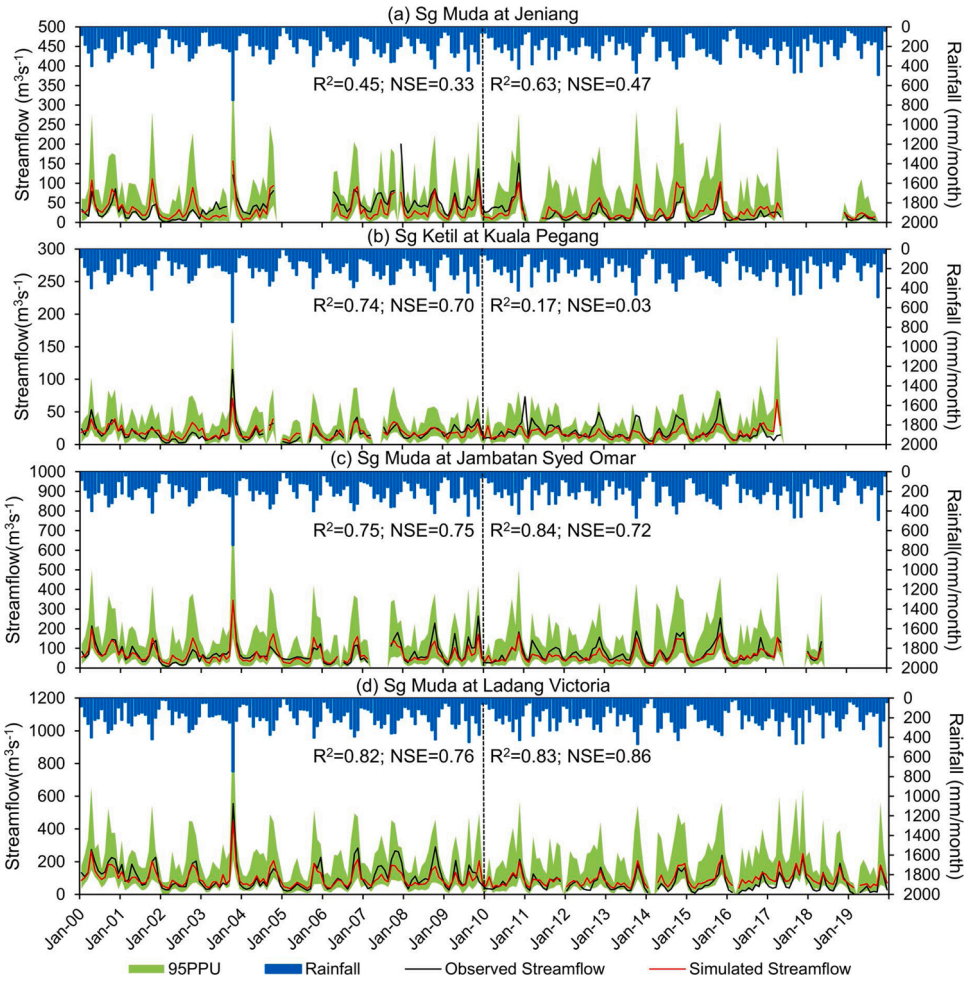

Fig. 6. SWAT Calibration and validation of monthly streamflow at the (a) Sg. Muda at Jeniang, (b) Sg. Ketil at Kuala Pegang, (c) Sg. Muda at Jambatan Syed Omar and (d) Sg. Muda at Ladang Victoria stations from 2000–2019. 95PPU is the 95 % prediction uncertainty that used to quantify the degree of uncertainty in the SWAT calibration and validation.

The SWAT calibration and validation indicated that it could capture the streamflow variability within an acceptable range in the MRB. However, lacking of observed data for surface runoff, groundwater and evapotranspiration resulted difficulty in identifying the SWAT performance on these water balance components. Based on the national water resources report prepared by DID (2011), the estimated annual groundwater recharge for the northern Peninsular Malaysia ranging from 120 to 130 mm/year, which is about 20–30 mm/year lower than the SWAT simulation. A larger difference (55–245 mm/year) between the SWAT-simulated groundwater (Nazri Ebrahim et al., 2020) and the national water resources report was found for the Kelantan River Basin that located in northeastern Peninsular Malaysia. A similar situation can be seen for the surface runoff and evapotranspiration components as well. In fact, streamflow is still regarded the only and most reliable source to test the performance of SWAT. Therefore, it is urgently need to install sensors that able to capture more water balance components for future validation work. Also, application of satellite-based evapotranspiration data for hydrological model calibration and validation is getting popular recently, particularly in ungauged or data-sparse basin (Jiang et al., 2020; Odusanya et al., 2019). This study emphasizes the need of developing a more comprehensive accuracy assessment of SWAT for other water balance components.

As mentioned early, the LULC scenarios doesn't have much impact on evapotranspiration, potential evapotranspiration and water yield of the MRB (Fig. 8). All the four LULC scenarios changed annual evapotranspiration, potential evapotranspiration and water yield by -0.64 to 0.57 %, 0.13 to 0.14 % and -0.99 to 0.07 %, respectively. A similar situation was found at the monthly scale assessment, with the changes mostly within 1–2%. A possible explanation by this might be that the LULC scenarios that set in this study is not significant enough to make significant changes in these three water balance components. In addition, since MRB is a tropical basin with high amount of precipitation, a reduction of few mm in these water balance components actually does not impact much on the overall amount. A similar finding was reported by Zhang et al. (2020b) in a tropical catchment of Australia, where the response of annual evapotranspiration to different LULC scenarios is within 0.3 %. Santos et al. (2018) also reported less significant changes in water components of a basin in Amazon due to the LULC changes, except surface runoff.

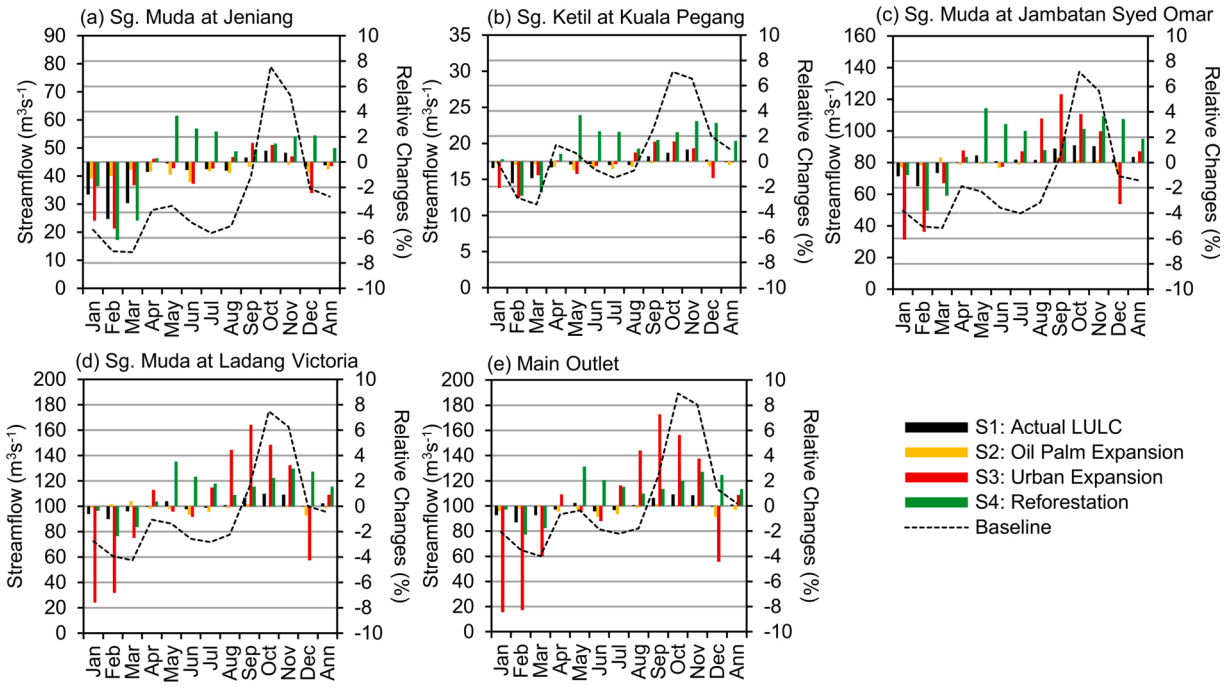

Fig. 7. Changes of average annual and monthly streamflow under various land use scenarios at (a) the Sg. Muda at Jeniang station, (b) the Sg. Ketil at Kuala Pegang station, (c) the Sg. Muda at Jambatan Syed Omar station, (d) the Sg. Muda at Ladang station and (e) basin outlet, during the period of 2000–2019.

Table 5
Annual relative changes of water balance components in Muda River Basin under various land use scenarios.

Water Balance Components	Baseline	S1 (%)	S2 (%)	S3 (%)	S4 (%)
Surface runoff (mm)	286.85	−0.17	0.79	34.51	−7.91
Lateral flow (mm)	470.50	−0.90	−3.52	−4.17	15.24
Groundwater (mm)	157.49	−5.80	−2.78	−18.84	6.83
Actual evapotranspiration (mm)	931.14	0.41	0.57	0.34	−0.66
Potential evapotranspiration (mm)	1521.01	0.13	0.14	0.14	0.14
Water yield (mm)	1455.74	−0.80	−0.99	−0.51	0.07
Streamflow (m^3s^{-1})	102.23	0.11	−0.29	0.87	1.35

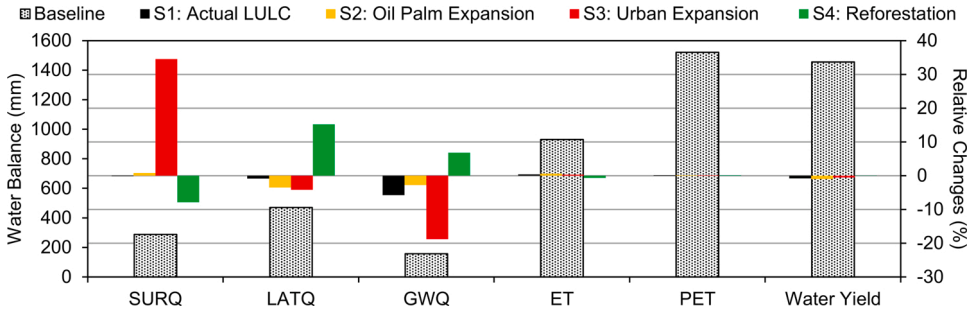

Fig. 8. Average annual changes of surface runoff (SURQ), lateral flow (LATQ), groundwater (GWQ), evapotranspiration (ET), potential evapotranspiration (PET) and water yield for different land use land cover scenarios in the Muda River Basin, Malaysia.

5. Conclusion

To obtain better LULC maps for tropical water balance analysis, this study proposed a framework to improve the ESA CCI LC products by integrating with freely available annual oil palm distribution images called AOPD (Xu et al., 2020). The framework is suitable for hydrologists with little or no experience in satellite images processing. The improved LULC products have been used to

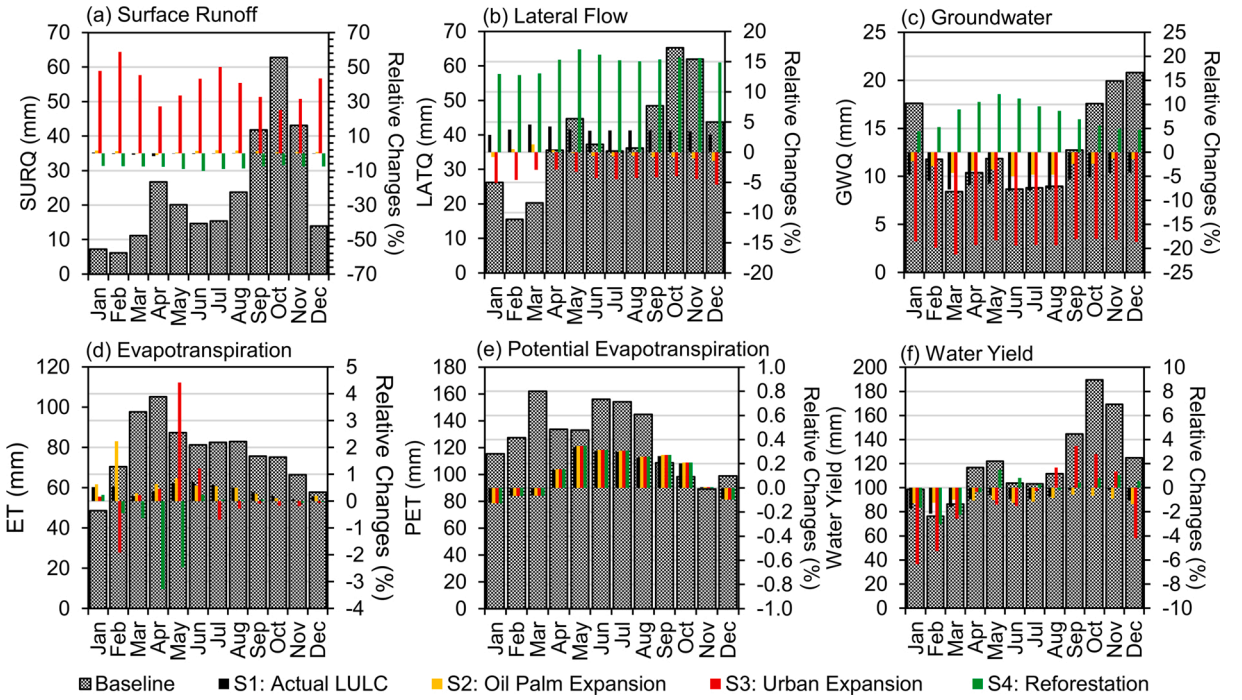

Fig. 9. Average monthly changes of (a) surface runoff (SURQ), (b) lateral flow (LATQ), (c) groundwater (GWQ), (d) evapotranspiration (ET), (e) potential evapotranspiration (PET) and (f) water yield for different land use land cover scenarios in the Muda River Basin, Malaysia.

generate the LULC maps for five different scenarios before incorporating into SWAT to study the impact of LULC changes on water balance in the MRB, Malaysia.

In general, the improved ESA CCI LC product can better represent the oil palm and rubber of the MRB compared to the original version. This indicates that a more comprehensive validation of global LULC products at local scale with more accurate ground truths should be conducted, particularly for the region with variety of LULC. During the 200–2016 period, the MRB experienced an oil palm expansion and a rubber reduction in the downstream region, whereas, forest in the northern and southeastern regions decreased slightly from 54.23%–52.80 %.

Consistent with previous studies (Tan et al., 2019a; Zhang et al., 2020a), SWAT performed well in monthly streamflow simulations in the MRB, with better performance can be found at the streamflow stations near to the basin outlets. CN2, ESCO and GW_REVAP are among the most sensitive parameters in the MRB that identified during the SWAT calibration. This study has shown that LULC changes have a larger impact on surface runoff, lateral flow and groundwater than actual evaporation, potential evapotranspiration, water yield and streamflow in the MRB. Basically, urban expansion will lead a significant increasing in surface runoff, which may result more serious floods. By contrast, reforestation is an effective strategy to reduce surface runoff, and increase lateral flow and groundwater recharge to the rivers. Oil palm expansion may lead to a reduction in lateral flow and groundwater due to the high soil water absorption capability as compared to rubber.

Future studies need to be carried out in order to validate more global LULC products in tropical regions. Besides that, improvement of these LULC products with other more specific datasets should be conducted and tested to produce more accurate LULC maps. Further research might explore the application of SWAT+ (Bieger et al., 2017), a newer SWAT version in streamflow simulations of tropical region. It would be interesting to see the performance of SWAT + compared to the SWAT model, particularly in extreme flows simulations (Tan et al., 2020).

CRediT authorship contribution statement

Mou Leong Tan: Conceptualization, Data curation, Formal analysis, Funding acquisition, Methodology, Writing - original draft. **Yi Lin Tew:** Methodology, Validation. **Kwok Pan Chun:** Writing - review & editing. **Narimah Samat:** Funding acquisition, Writing - review & editing. **Shazlyn Milleana Shaharudin:** Funding acquisition, Writing - review & editing. **Mohd Amirul Mahamud:** Methodology, Validation. **Fredolin T. Tangang:** Funding acquisition, Writing - review & editing.

Declaration of Competing Interest

The authors report no declarations of interest.

Acknowledgements

This research was funded by the Ministry of Higher Education Malaysia under Long-term Research Grant Scheme project 2, grant number LRGS/1/2020/UKM-USM/01/6/2 which is under the program of LRGS/1/2020/UKM/01/6. This research was supported in part with Kurita Asia Research Grant (20Pmy024-K19) provided by Kurita Water and Environment Foundation.

Thanks to the Malaysian Meteorological Department (MMD), Department of Irrigation and Drainage (DID) Malaysia, Ministry of Agriculture and Agro-based Industry Malaysia (MOA), Muda Agricultural Development Authority (MADA) for providing data that required in the model development. Special thanks to the ESA CCI LC, AOPD, SRTM, FAO and SWAT developers for distributing their data and tool freely to the public.

Appendix A. Supplementary data

Supplementary material related to this article can be found, in the online version, at doi:https://doi.org/10.1016/j.ejrh.2021.100837.

References

Abbaspour, K.C., Vaghefi, S.A., Srinivasan, R., 2018. A guideline for successful calibration and uncertainty analysis for soil and Water assessment: a review of papers from the 2016 International SWAT Conference. Water 10 (1), 18. https://doi.org/10.3390/w10010006.

Arnold, J.G., Srinivasan, R., Muttiah, R.S., Williams, J.R., 1998. Large area hydrologic modeling and assessment part I: model development. JAWRA J. Am. Water Resour. Assoc. 34 (1), 73–89. https://doi.org/10.1111/j.1752-1688.1998.tb05961.x.

Bartholomé, E., Belward, A.S., 2005. GLC2000: a new approach to global land cover mapping from earth observation data. Int. J. Remote Sens. 26 (9), 1959–1977. https://doi.org/10.1080/01431160412331291297.

Bieger, K., et al., 2017. Introduction to SWAT+, a completely restructured version of the soil and water assessment tool. JAWRA J. Am. Water Resour. Assoc. 53 (1), 115–130. https://doi.org/10.1111/1752-1688.12482.

Bressiani, D.A., et al., 2015. Review of soil and water assessment tool (SWAT) applications in Brazil: challenges and prospects. Int. J. Agric. Biol. Eng. 8 (3), 9–35. https://doi.org/10.3965/j.ijabe.20150803.1765.

Chen, Y., et al., 2020. Study on streamflow response to land use change over the upper reaches of zhanghe Reservoir in the Yangtze River basin. Geosci. Lett. 7 (1), 6. https://doi.org/10.1186/s40562-020-00155-7.

Chirachawala, C., Shrestha, S., Babel, M.S., Virdis, S.G.P., Wichakul, S., 2020. Evaluation of global land use/land cover products for hydrologic simulation in the Upper Yom River Basin, Thailand. Sci. Total Environ. 708, 135148 https://doi.org/10.1016/j.scitotenv.2019.135148.

Cohen, J., 1960. A coefficient of agreement for nominal scales. Educ. Psychol. Meas. 20 (1), 10. DOI:https://doi.org/10.1177%2F001316446002000104.

Defourny, P., et al., 2016. Land Cover CCI: Product User Guide Version 2.

DID, 2011. Review of the National Water Resources (2000-2050) and Formulation of National Water Resources Policy - Volume 2 Water Resources Givernance, Final Report.

DID, 2020. National Water Balance Management System.

ESA, 2017. Land Cover CCI Product User Guide Version 2. Tech. Rep.

FAO, 2010. Food and agriculture organization of the United Nations, 2010. Global Forest Resources Assessment 2010.

FOMCA, Fo.M.C.A., 2009. A Study Report on Groundwater Resources Development Project in the District of Batang Padang, Perak Darul Ridzuan: A Reminder to Malaysia. Federation of Malaysian Consumers Associations (FOMCA).

Foody, G.M., 2010. Assessing the accuracy of land cover change with imperfect ground reference data. Remote Sens. Environ. 114 (10), 15. https://doi.org/10.1016/j.rse.2010.05.003.

Foody, G.M., 2015. Valuing map validation: the need for rigorous land cover map accuracy assessment in economic valuations of ecosystem services. Ecol. Econ. 111, 6. https://doi.org/10.1016/j.ecolecon.2015.01.003.

Gassman, P.W., Wang, Y., 2015. IJABE SWAT Special issue: innovative modeling solutions for water resource problems. Int. J. Agric. Biol. Eng. 8 (3), 1–8. https://doi.org/10.3965/j.ijabe.20150803.176.

Gassman, P.W., Reyes, M.R., Green, C.H., Arnold, J.G., 2007. The soil and Water assessment tool: historical development, applications, and future research directions. Trans. ASABE 50 (4), 1211–1250. https://doi.org/10.13031/2013.23637.

Gassman, P.W., Sadeghi, A.M., Srinivasan, R., 2014. Applications of the SWAT model Special section: overview and insights. J. Environ. Qual. 43 (1), 1–8. https://doi.org/10.2134/jeq2013.11.0466.

Githui, F., Mutua, F., Bauwens, W., 2009. Estimating the impacts of land-cover change on runoff using the soil and water assessment tool (SWAT): case study of Nzoia catchment, Kenya. Hydrol. Sci. J. 54 (5), 899–908. https://doi.org/10.1623/hysj.54.5.899.

Hansen, M.C., Stehman, S.V., Potapov, P.V., 2010. Quantification of global gross forest cover loss. Proc. Natl. Acad. Sci. 107 (19), 8650–8655. https://doi.org/10.1073/pnas.0912668107.

Hardanto, A., et al., 2017. Oil Palm and rubber tree Water use patterns: effects of topography and flooding. Front. Plant Sci. 8 https://doi.org/10.3389/fpls.2017.00452, 452-452.

Jiang, L., et al., 2020. Satellite-based evapotranspiration in hydrological model calibration. Remote Sensing 12 (3), 428.

Jourdan, C., Michaux-Ferriere, N., Perbal, G., 2000. Root system architecture and gravitropism in the oil palm. Ann. Bot. 85 (6), 861–868. https://doi.org/10.1006/anbo.2000.1148.

Kondo, T., Sakai, N., Yazawa, T., Shimizu, Y., 2021. Verifying the applicability of SWAT to simulate fecal contamination for watershed management of Selangor River, Malaysia. Sci. Total Environ. 145075. https://doi.org/10.1016/j.scitotenv.2021.145075.

Li, W., et al., 2016. Major forest changes and land cover transitions based on plant functional types derived from the ESA CCI Land cover product. Int. J. Appl. Earth Obs. Geoinf. 47, 30–39. https://doi.org/10.1016/j.jag.2015.12.006.

Lyons, M.B., Keith, D.A., Phinn, S.R., Mason, T.J., Elith, J., 2018. A comparison of resampling methods for remote sensing classification and accuracy assessment. Remote Sens. Environ. 208, 9. https://doi.org/10.1016/j.rse.2018.02.026.

MADA, 2020. Information of MADA's Dams.

Malingreau, J.P., Tucker, C.J., Laporte, N., 1989. AVHRR for monitoring global tropical deforestation. Int. J. Remote Sens. 10 (4-5), 855–867. https://doi.org/10.1080/01431168908903926.

Mannschatz, T., Wolf, T., Hülsmann, S., 2016. Nexus tools platform: web-based comparison of modelling tools for analysis of water-soil-waste nexus. Environ. Modell. Software 76, 137–153. https://doi.org/10.1016/j.envsoft.2015.10.031.

Moriasi, D.N., Gitau, M.W., Pai, N., Daggupati, P., 2015. Hydrologic and water quality models: performance measures and evaluation criteria. Trans. ASABE 58 (6), 1763–1785. https://doi.org/10.13031/trans.58.10715.
Moriasi, D.N., et al., 2019. SWAT-LUT: a desktop graphical user interface for updating land use in SWAT. JAWRA J. Am. Water Resour. Assoc. 55 (5), 1102–1115. https://doi.org/10.1111/1752-1688.12789.
Mousivand, A., Arsanjani, J.J., 2019. Insights on the historical and emerging global land cover changes: the case of ESA-CCI-LC datasets. Appl. Geogr. 106, 82–92. https://doi.org/10.1016/j.apgeog.2019.03.010.
Nazri, Ebrahim, Mohamed Azwan, M.Z., Md Rowshon, K., K, N, 2020. Evaluation of groundwater recharge based on climate change: a case study at Baung's watershed, Kota Bharu, Kelantan. Sains Malaysiana 49 (11), 2649–2658.
Nilawar, A.P., Waikar, M.L., 2018. Use of SWAT to determine the effects of climate and land use changes on streamflow and sediment concentration in the Purna River basin, India. Environ. Earth Sci. 77 (23), 783. https://doi.org/10.1007/s12665-018-7975-4.
Nowosad, J., Stepinski, T.F., Netzel, P., 2019. Global assessment and mapping of changes in mesoscale landscapes: 1992–2015. Int. J. Appl. Earth Obs. Geoinf. 78, 332–340. https://doi.org/10.1016/j.jag.2018.09.013.
Odusanya, A.E., et al., 2019. Multi-site calibration and validation of SWAT with satellite-based evapotranspiration in a data-sparse catchment in southwestern Nigeria. Hydrol. Earth Syst. Sci. 23 (2), 1113–1144. https://doi.org/10.5194/hess-23-1113-2019.
Olofsson, P., et al., 2014. Good practices for estimating area and assessing accuracy of land change. Remote Sens. Environ. 148, 16. https://doi.org/10.1016/j.rse.2014.02.015.
Pai, N., Saraswat, D., 2011. SWAT2009_LUC: a tool to activate the land use change module in SWAT 2009. Trans. ASABE 54 (5), 1649–1658. https://doi.org/10.13031/2013.39854.
Plummer, S., Lecomte, P., Doherty, M., 2017. The ESA climate change initiative (CCI): a European contribution to the generation of the global climate observing system. Remote Sens. Environ. 203, 2–8. https://doi.org/10.1016/j.rse.2017.07.014.
Reinhart, V., et al., 2021. Comparison of ESA climate change initiative land cover to CORINE land cover over Eastern Europe and the Baltic States from a regional climate modeling perspective. Int. J. Appl. Earth Obs. Geoinf. 94, 102221 https://doi.org/10.1016/j.jag.2020.102221.
Santos, C.A.S., et al., 2018. Using a hierarchical approach to calibrate SWAT and predict the semi-arid hydrologic regime of northeastern Brazil. Water 10 (9), 1137.
Schilling, K.E., Jha, M.K., Zhang, Y.-K., Gassman, P.W., Wolter, C.F., 2008. Impact of land use and land cover change on the water balance of a large agricultural watershed: historical effects and future directions. Water Resour. Res. 44 (7) https://doi.org/10.1029/2007WR006644.
Stibig, H.J., Achard, F., Carboni, S., Raši, R., Miettinen, J., 2014. Change in tropical forest cover of Southeast Asia from 1990 to 2010. Biogeosciences 11 (2), 247–258. https://doi.org/10.5194/bg-11-247-2014.
Sulla-Menashe, D., Friedl, M.A., 2018. User Guide to Collection 6 MODIS Land Cover (MCD12Q1 and MCD12C1) Product. USGS, Reston, VA, USA.
Tamm, O., Maasikamäe, S., Padari, A., Tamm, T., 2018. Modelling the effects of land use and climate change on the water resources in the eastern Baltic Sea region using the SWAT model. CATENA 167, 78–89. https://doi.org/10.1016/j.catena.2018.04.029.
Tan, M.L., Ibrahim, A.L., Yusop, Z., Duan, Z., Ling, L., 2015. Impacts of land-use and climate variability on hydrological components in the Johor River basin, Malaysia. Hydrol. Sci. J. 60 (5), 873–889. https://doi.org/10.1080/02626667.2014.967246.
Tan, M.L., Gassman, P.W., Srinivasan, R., Arnold, J.G., Yang, X., 2019a. A review of SWAT studies in Southeast Asia: applications, challenges and future directions. Water 11 (5), 914. https://doi.org/10.3390/w11050914.
Tan, M.L., Samat, N., Chan, N.W., Lee, A.J., Li, C., 2019b. Analysis of precipitation and temperature extremes over the Muda River Basin, Malaysia. Water 11 (2), 283. https://doi.org/10.3390/w11020283.
Tan, M.L., Gassman, P., Yang, X., Haywood, J., 2020. A review of SWAT applications, performance and future needs for simulation of hydro-climatic extremes. Adv. Water Resour. 143, 103662 https://doi.org/10.1016/j.advwatres.2020.103662.
Tangang, F., et al., 2017. Characteristics of precipitation extremes in Malaysia associated with El Niño and La Niña events. Int. J. Climatol. 37 (S1), 696–716. https://doi.org/10.1002/joc.5032.
Tapia, J.F.D., Doliente, S.S., Samsatli, S., 2021. How much land is available for sustainable palm oil? Land Use Policy 102, 105187. https://doi.org/10.1016/j.landusepol.2020.105187.
UN, 2020. Population.
van Griensven, A., Ndomba, P., Yalew, S., Kilonzo, F., 2012. Critical review of SWAT applications in the Upper Nile basin countries. Hydrol. Earth Syst. Sci. 16, 3371–3381.
Van Kalken, T., 2017. Malaysian national Water balance system (NAWABS) for improved River Basin management: case study in the Muda River Basin. In: E-Proceedings of the 37th IAHR World Congress. August 13–18, 2017, Kuala Lumpur, Malaysia.
Wulder, M.A., Franklin, S.E., White, J.C., Linke, J., Magnussen, S., 2006. An accuracy assessment framework for large-area land cover classification products derived from medium-resolution satellite data. Int. J. Remote Sens. 27 (4), 21. https://doi.org/10.1080/01431160500185284.
Xu, Y., et al., 2020. Annual oil palm plantation maps in Malaysia and Indonesia from 2001 to 2016. Earth Syst. Sci. Data 12 (2), 847–867. https://doi.org/10.5194/essd-12-847-2020.
Zhang, D., et al., 2020a. Comparison of NCEP-CFSR and CMADS for hydrological modelling using SWAT in the Muda River Basin, Malaysia. Water 12 (11), 3288.
Zhang, H., et al., 2020b. Using an improved SWAT model to simulate hydrological responses to land use change: a case study of a catchment in tropical Australia. J. Hydrol. 585, 124822 https://doi.org/10.1016/j.jhydrol.2020.124822.